

## Shape transitional aspects of odd-*A* Eu isotopes studied by the (*p*, *t*) reaction\*

H. Taketani,<sup>†</sup> H. L. Sharma,<sup>‡</sup> and Norton M. Hintz

*J. H. Williams Laboratory of Nuclear Physics, University of Minnesota, Minneapolis, Minnesota 55455*

(Received 17 December 1974; revised manuscript received 31 March 1975)

The abrupt shape transition as is observed around  $N \simeq 88-90$  in even nuclei has been examined for the odd-*A* Eu isotopes  $^{151}\text{Eu}_{88}$  and  $^{149}\text{Eu}_{86}$  by the (*p*, *t*) reaction at 18.5 and 19.0 MeV with an average resolution of 10 keV. Angular distributions, taken from 10 to 70°, enabled unambiguous identification of many  $L = 0$  ( $J_f^\pi = 5/2^+$ ) transitions in both residual nuclei; seven for  $^{151}\text{Eu}$  and seven or eight for  $^{149}\text{Eu}$ . The summed  $L = 0$  cross sections are close to those of the (*p*, *t*) reactions for the neighboring even-*A* Sm isotopes connecting the same neutron numbers. A number of new levels have been found in both isotopes. We have obtained markedly different level structures for the two neighboring isotoopes. In  $^{151}\text{Eu}$ , whose ground state and low-lying states below 200 keV can be described in terms of spherical shell-model configurations, two deformed bands have been tentatively identified. One of these is a  $5/2^+[413]$  band with members at 261 keV,  $5/2^+$ ; 414 keV,  $(7/2^+)$ ; and possibly a 597 keV,  $(9/2^+)$  member. In addition a  $5/2^+[413]$   $\beta$  band is postulated with members at 654 keV,  $5/2^+$ ; 801 keV,  $(7/2^+)$ . These deformed states, coexisting with the spherical states, have been strongly excited while the spherical low-lying states have shown vanishingly small (*p*, *t*) cross sections. The (*p*, *t*) cross sections to the  $^{151}\text{Eu}$  states were found to be in strong anticorrelation with  $B(E2)$  values from Coulomb excitation and (*d*, *d'*) cross sections leading to the same final states. On the other hand,  $^{149}\text{Eu}$  has shown the usual (*p*, *t*) pattern of a strong ground state transition and weak excited state transitions, showing similar coupling schemes are involved in the ground states of  $^{151}\text{Eu}$  and  $^{149}\text{Eu}$ . The detailed experimental results up to 1.6 MeV excitation in both nuclei and their interpretation for some of the levels are presented.

[NUCLEAR REACTIONS  $^{153,151}\text{Eu}(p, t)$ ,  $E = 18.5$  and  $19.0$  MeV; measured  $\sigma(E_t, \theta)$ ,  $Q$ .  $^{151,149}\text{Eu}$  deduced levels,  $J, \pi$ . Enriched targets.]

### I. INTRODUCTION

The (*p*, *t*) and (*t*, *p*) reactions connecting two even-even isotopes have shown special features for the nuclei Nd, Sm, and Gd in the well known shape transition region around  $N = 88-90$ .<sup>1-12</sup> In a typical example, the (*p*, *t*) reaction  $^{152}\text{Sm}_{90}(p, t)-^{150}\text{Sm}_{88}$ <sup>7</sup> shows comparable  $L = 0$  transfer strengths for three  $0^+$  states in  $^{150}\text{Sm}$ : the ground, 738, and 1255 keV states. The 1255 keV state is generally interpreted as a deformed state, to which the strong two-neutron transfer can occur from the deformed (prolate) ground state of  $^{152}\text{Sm}$ . A similar pattern of intensities had been seen previously<sup>1,2</sup> in the reaction  $^{150}\text{Sm}(t, p)^{152}\text{Sm}$ , indicating a state in  $^{152}\text{Sm}$  at 1091 keV is mainly spherical. However, the distinction between "spherical" and "deformed" is by no means clear in the above cases, as seen in the comparable splitting of the  $L = 0$  transfer strength into three low-lying states. The Kumar-Baranger picture of large zero-point oscillations<sup>13</sup> is usually employed to account for such a strong mixing of low-lying  $0^+$  states.

It is interesting to investigate the corresponding (*p*, *t*) reaction processes in the odd-proton isotones  $^{153}\text{Eu}_{90}(p, t)^{151}\text{Eu}_{88}$  and  $^{151}\text{Eu}_{88}(p, t)^{149}\text{Eu}_{86}$ , to determine the effect of the odd proton on the deformed and vibrational states of the core. It is known that  $^{153}\text{Eu}$  has a large static quadrupole

moment<sup>14</sup> and a ground-state rotational band<sup>15</sup> characteristic of a deformed nucleus. For the nucleus  $^{151}\text{Eu}$  there is no ground-state rotational band observed, and the ground state has a much smaller static quadrupole moment than  $^{153}\text{Eu}$ .<sup>14</sup> All three Eu isotopes,  $^{153}\text{Eu}$ ,  $^{151}\text{Eu}$ , and  $^{149}\text{Eu}$ , of the present investigation have a ground-state spin-parity of  $\frac{5}{2}^+$ , and the two adjacent ground states may be connected with predominantly  $L = 0$  transfers, thus enabling a straightforward comparison of the  $L = 0$  intensity patterns with those for even-even nuclei.

The low-lying levels of  $^{151}\text{Eu}$  have been previously investigated by several methods. Zavadil and Graetzer,<sup>16</sup> using Coulomb excitation by  $\alpha$  particles, have deduced the  $^{151}\text{Eu}$  levels up to 1106 keV. Lewis and Graetzer<sup>17</sup> have investigated the  $^{151}\text{Eu}$  levels to 906 keV by measuring the de-excitation  $\gamma$  rays following Coulomb excitation by protons and  $\alpha$  particles. Thun and Miller<sup>18</sup> have assigned spins and parities of levels up to 503.5 keV from Coulomb excitation studies using  $\alpha$  particles and  $^{35}\text{Cl}$  ions. Boss<sup>19</sup> and Bernstein *et al.*,<sup>20</sup> using inelastic scattering of deuterons, have studied  $^{151}\text{Eu}$  levels up to an excitation energy of 1163 keV and have observed those levels populated by  $L = 2$  or  $L = 3$  transitions. Beside these reaction studies, the  $^{151}\text{Eu}$  levels below 416 keV have been investigated in the decay of  $^{151}\text{Gd}$ .<sup>21,22</sup> In spite of the

many experiments published before 1973, there has been no positive evidence for the existence of deformed states in  $^{151}\text{Eu}$ . In contrast to  $^{151}\text{Eu}$ , the only data available for  $^{149}\text{Eu}$  are those from the decay of  $^{149}\text{Gd}$ .<sup>23-27</sup> After this experiment was completed, Burke *et al.* published evidence for shape coexistence in  $^{151}\text{Eu}$  from the  $^{153}\text{Eu}(p, t)^{151}\text{Eu}$  reaction at 18 MeV,<sup>28</sup> which is quite similar to ours for  $^{151}\text{Eu}$ . A preliminary account of the present paper has also been reported at the Munich Conference.<sup>29</sup>

## II. EXPERIMENTAL PROCEDURE

An 18.5 MeV proton beam was obtained from the J. H. Williams Laboratory MP tandem Van de Graaff. Due to technical difficulties encountered in accelerator operation, complete angular distributions from  $\theta_{\text{lab}} = 10$  to  $70^\circ$  could be taken only at 18.5 MeV. The measurements were repeated later for seven angles at 19.0 MeV, in order to compare the cross sections with those of the  $^{152, 150}\text{Sm}(p, t)^{150, 148}\text{Sm}$  reactions which had been investigated previously at 19.0 MeV.<sup>7</sup> The outgoing tritons were detected with an Enge split-pole spectrograph with position sensitive detectors (PSD) in the focal plane.<sup>30</sup> Position information was obtained with an on-line computer by dividing the energy-times-position ( $\times E$ ) signal by the energy ( $E$ ) signal from each of the PSD's. The  $E$  signals were also used for particle identification. The over-all energy resolution including the effect of target thickness was  $\sim 10$  keV full width at half-maximum (FWHM) for both isotopes. Isotopically enriched Eu targets of thicknesses  $108 \mu\text{g}/\text{cm}^2$  (98.76%  $^{153}\text{Eu}$ ) and  $71 \mu\text{g}/\text{cm}^2$  (96.83%  $^{151}\text{Eu}$ ) were made by reduction evaporation of enriched  $\text{Eu}_2\text{O}_3$ <sup>31</sup> onto  $30 \mu\text{g}/\text{cm}^2$  thick carbon backings. The target material was evaporated using a resistively heated Ta boat with powdered Ti serving as the reducing agent. The thicknesses of the enriched targets were determined by measuring the yields, with a known solid angle, of the elastic scattering of 8 MeV protons at forward angles ( $\sim 50$ – $65^\circ$ ), and by assuming the cross sections were equal to those for Rutherford scattering. According to the optical-model predictions, deviations from pure Coulomb scattering cross sections at  $\theta_{\text{lab}} < 65^\circ$  are within  $\pm 1.5\%$  for the elastic scattering of 8 MeV protons on Eu. The  $(p, t)$  measurements were made also for natural targets ( $^{153}\text{Eu}$ : 52.14%,  $^{151}\text{Eu}$ : 47.86%) in order to determine the precise cross-section ratios of the two isotopes.

## III. EXPERIMENTAL RESULTS

### A. General

The  $Q$  values for the strongest  $L=0$  transitions were determined by comparison with reactions of

known  $Q$  value. Excitation energies of the residual nuclear levels were determined with calibration constants (energy vs position) for the PSD's obtained by positioning the elastic peak and/or the  $^{151}\text{Eu}(p, t)^{149}\text{Eu}$  g.s. peak at several different locations on the spectrograph focal plane by varying the magnetic field. Results quoted are averages for 14 angles measured. Estimated errors are  $\pm 5$  keV for absolute  $Q$  values and  $\pm 3$  keV for excitation energies.

The  $(p, t)$  absolute cross sections were obtained using the target thicknesses determined by the elastic scattering of 8 MeV protons, as described in the previous section, and the known spectrometer geometry. The errors in the absolute cross sections for the 261 keV state transition of the  $^{153}\text{Eu}(p, t)^{151}\text{Eu}$  reaction and for the ground-state transition of the  $^{151}\text{Eu}(p, t)^{149}\text{Eu}$  reaction are estimated to be  $\pm 10\%$ , respectively, at  $\theta_{\text{lab}} = 25^\circ$  near the  $L=0$  maxima. Relative errors are shown in the figures.

As is well known, the angular distributions from  $(p, t)$  reactions, at least at energies  $\lesssim 25$  MeV, generally give unambiguous assignments of the transferred  $L$  value only for  $L=0$ . For other  $L$  values the angular distributions tend to be without pronounced structure, and are sensitive to the configurations involved in the transfer as well as to higher order multistep processes.<sup>12, 32-35</sup> In addition to the above ambiguities, more complexities arise from the possible  $L$  admixtures due to the nonzero spin of the odd- $A$  target nucleus. [For  $(p, t)$  reactions the following approximate selection rules hold:  $|J_i - J_f| \leq L \leq J_i + J_f$ ,  $\pi_i \pi_f = (-1)^L$ . There is an additional  $K$ -selection rule for deformed nuclei:  $|K_i - K_f| \leq L$ .] However, if an  $L=0$  angular distribution is observed, then  $J_f = J_i$  in almost all cases. Under such circumstances, the main effort was concentrated in finding  $L=0$ , and hence  $J^\pi = \frac{5}{2}^+$  levels. From clear  $L=0$  patterns seven or eight  $\frac{5}{2}^+$  states were unambiguously identified in both nuclei. Definite assignments for other spins are very difficult to make from  $(p, t)$  angular distributions alone. However, we have made tentative assignments of  $J^\pi = \frac{7}{2}^+$  for two levels in the present investigation, relying partly on energy and upon well established intensity systematics within rotational bands.<sup>36</sup>

### B. $^{153}\text{Eu}(p, t)^{151}\text{Eu}$

A typical triton spectrum is shown in Fig. 1. The  $Q$  value for the ground-state transition was found to be  $-6.374 \pm 0.005$  MeV, in agreement with the previously quoted value of  $-6.378 \pm 0.004$  MeV.<sup>37</sup> The triton angular distributions are shown in Figs. 2(a)–2(c). From these angular distributions,

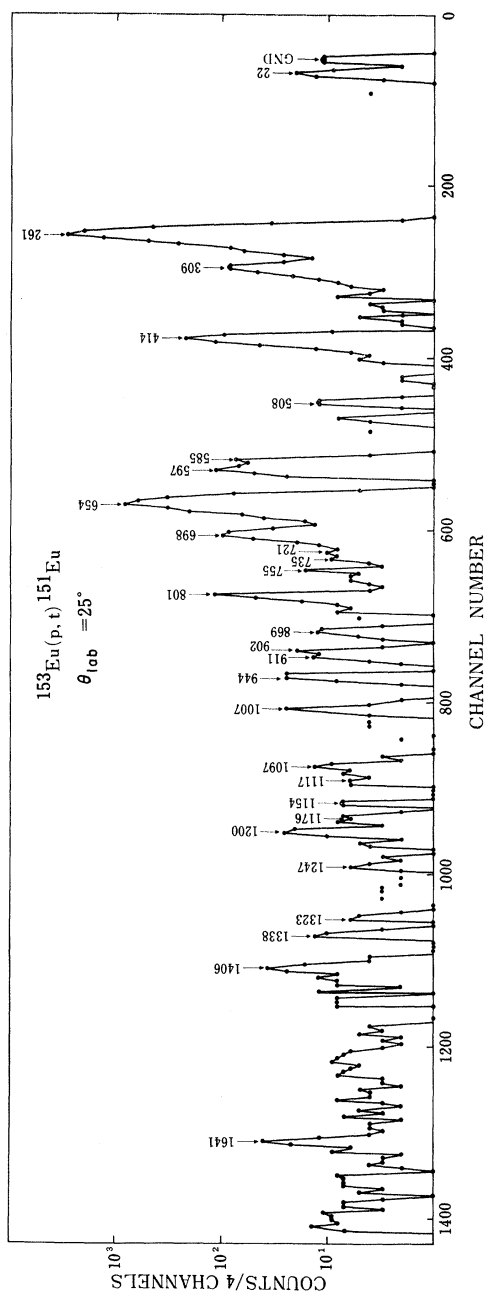


FIG. 1. A typical triton PSD spectrum for the  $^{153}\text{Eu}(p, t)^{151}\text{Eu}$  reaction at  $E_p = 18.5$  MeV and  $\theta_{\text{lab}} = 25^\circ$ . The sums of counts for every four channels are plotted. Energies for the states are given in keV.

unambiguous  $L=0$  ( $J^\pi = \frac{5}{2}^+$ ) assignments were made for seven states (energies in keV): the ground, 261, 309 (doublet?), 585, 654, 698, and 902 keV states in  $^{151}\text{Eu}$ . Tentative  $\frac{7}{2}^+$  assignments were made for the 414 and 801 keV states which have nearly identical angular distributions. Further reasons for the speculative assignment of  $J^\pi = \frac{7}{2}^+$  for the 414 and 801 keV states are given in Sec. IV A. In Table I, excitation energies, peak cross sections, transferred  $L$  values, and assigned spins and parities of the  $^{151}\text{Eu}$  levels up to 1641 keV are summarized, together with assignments from other experiments.

### C. $^{151}\text{Eu}(p, t)^{149}\text{Eu}$

A typical triton spectrum is shown in Fig. 3. The  $Q$  value for the ground-state transition was found to be  $-5.872 \pm 0.005$  MeV. This is the first direct measurement of this  $Q$  value and the present result is 58 keV less negative than the previously quoted value of  $-5.930$  MeV,<sup>37</sup> which was estimated from  $\beta$ -decay energy systematics. The angular distributions are shown in Figs. 4(a)–4(c). Seven and possibly eight  $\frac{5}{2}^+$  states were identified from these angular distributions ( $L=0$ ): the ground, 754, 879, 955, 1150, 1226, 1319, and possibly the 1064 keV states. In Table II, excitation energies, peak cross sections, transferred  $L$  values, and spins and parities are shown for the  $^{149}\text{Eu}$  levels up to 1555 keV, together with the previous  $^{149}\text{Gd}$  decay assignments.

### D. DWBA analysis

Since the wave functions of the residual states and their inelastic transition matrix elements are not well known, only a naive distorted wave Born approximation (DWBA) calculation was performed to get a rough idea of the  $L$  values involved in each transition. For low-lying states of the residual nuclei studied in the present experiment, the relevant Nilsson orbits of neutrons are mostly those originating from the  $2f_{7/2}$ ,  $1h_{9/2}$ , and  $1i_{13/2}$  shell-model orbits in their spherical limits. Calculations were made for pure spherical shell-model configurations with various combinations of two of the above orbits for the bound-state wave functions of the transferred neutron pair. Although the calculation gave an order of magnitude higher cross sections for any configuration in which at least one neutron occupied the  $2f_{7/2}$  orbit in a given  $L$  transfer, the calculated shape of the angular distribution was found to be rather insensitive to the choice of the configuration. Therefore, for each pure  $L$  transfer, the angular distribution calculated with the configuration of either  $(2f_{7/2})^2_\nu$  (for  $L=0, 2, 4,$  and  $6$ ) or  $(2f_{7/2}, 1i_{13/2})_\nu$

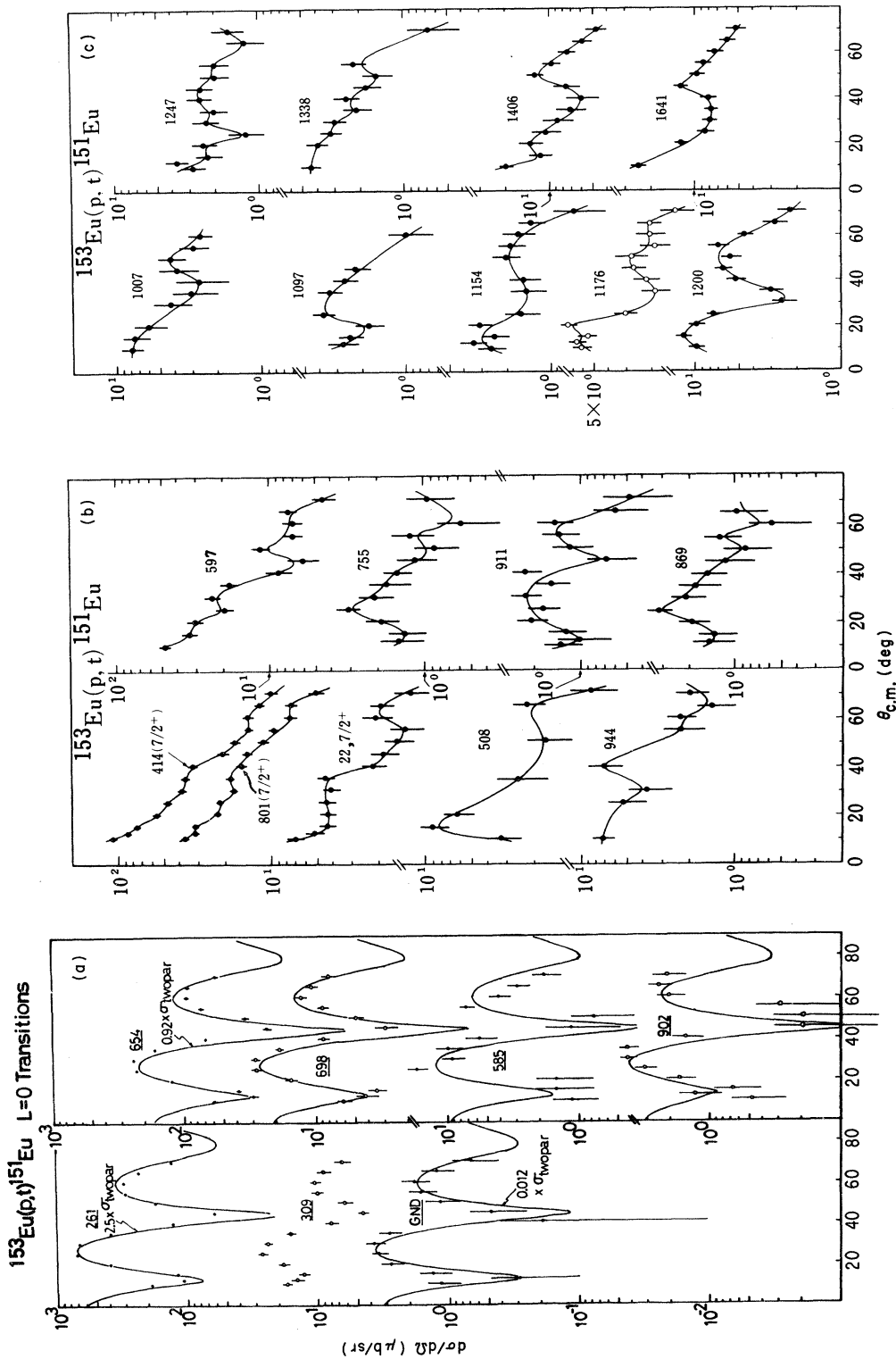


FIG. 2. (a) The  $L=0$  angular distributions for the  $^{153}\text{Eu}(p,t)^{151}\text{Eu}$  reaction at 18.5 MeV. Energies of the states are given in keV. Solid curves show the arbitrarily normalized DWBA fits using the code TWOPAR (Ref. 38). For these curves, the bound-state wave functions of the transferred neutrons are assumed to be due to the  $(2f_{7/2})^2_\nu$  shell-model configuration. Normalization factors for the DWBA cross sections are indicated for the ground, 261, and 654 keV states. (b), (c) Angular distributions for the  $^{153}\text{Eu}(p,t)^{151}\text{Eu}$  reaction. Energies are given in keV. Each of the solid curves serves only as a guide to the eye.

TABLE I. Level properties of  $^{151}\text{Eu}$  from the present ( $E_p = 18.5$  MeV) and other experiments. See Sec. IIIA for the errors in the present experiment.

$E_x$ (keV)	$^{150}\text{Eu}(\beta, t)^a$ Present exp.		$^{153}\text{Eu}(\beta, t)^b$		Coulomb exc. c		Coulomb exc. d		Coulomb exc. e		Inel. scatt. f		Decay of $^{151}\text{Gd}^g$		Decay of $^{151}\text{Gd}^h$	
	$\sigma(\theta)_{\text{max}}$ ( $\mu\text{b}/\text{sr}$ )	$\theta_{\text{lab}}$ (deg)	$E_x$ (keV)	$\sigma(30^\circ)$ ( $\mu\text{b}/\text{sr}$ )	$L$	$J^\pi$	$E_x$ (keV)	$J^\pi$	$E_x$ (keV)	$J^\pi$	$E_x$ (keV)	$J^\pi$	$E_x$ (keV)	$J^\pi$	$E_x$ (keV)	$J^\pi$
0	3.7	30	0	4	0	$\frac{5}{2}^+$	0	$\frac{5}{2}^+$	0	$\frac{5}{2}^+$	0	0	$\frac{5}{2}^+$	0	$\frac{5}{2}^+$	$\frac{5}{2}^+$
22	7.1	10	22			$\frac{7}{2}^{+*}$	21.6	$\frac{7}{2}^+$	21.54	$\frac{7}{2}^+$	0	21.6	$\frac{7}{2}^+$	21.54	$\frac{7}{2}^+$	$\frac{7}{2}^+$
261	712.9	25	261	487	0	$\frac{5}{2}^+$	195.8	$\frac{1}{2}^+$	196.21	$\frac{11}{2}^-$	196	196.6	$\frac{11}{2}^-$	196.21	$\frac{11}{2}^-$	$\frac{11}{2}^-$
309	26.9	25	307	$\sim 17$	0	$\frac{5}{2}^+ + (\frac{3}{2}^+)^*$	196.5	$\frac{11}{2}^-$	196.45	$\frac{3}{2}^+$		243.6	$\frac{5}{2}^+, \frac{7}{2}^-$	196.46	$(\frac{1}{2})^+$	$(\frac{1}{2})^+$
(doublet)			(doublet)				243.0	$(\frac{7}{2}^-)$	243.1	$\frac{7}{2}^-$		260.8	$\frac{3}{2}^+, \frac{5}{2}^+, \frac{7}{2}^+$	243.22	$\frac{7}{2}^-$	$(\frac{3}{2}^- - \frac{9}{2}^-)^+$
414	104.8	10	415			$(\frac{7}{2}^+)$	306.8	$\frac{3}{2}^+$	307.0		307	308.0	$\frac{5}{2}^+, \frac{7}{2}^+$	307.47	$(\frac{3}{2}^- - \frac{7}{2}^-)^+$	$(\frac{3}{2}^- - \frac{7}{2}^-)^+$
508	9.0	15					500		499.6		503	350.3	$\frac{9}{2}^-$	349.76	$\frac{9}{2}^-$	$\frac{9}{2}^-$
585	17.1	25	587	10	0	$\frac{5}{2}^+$	580		503.5	$\frac{9}{2}^+$	588	354.2	+	353.56	$\frac{5}{2}^-, \frac{7}{2}^-$	$\frac{5}{2}^-, \frac{7}{2}^-$
597	48.1	10	600				604		600.6		602	416.3				
654	242.4	30	653	176	0	$\frac{5}{2}^+$										
698	28.5	30	696	23	0	$\frac{5}{2}^+$	(696)				701					
721							718		719		720					
735											758					
755	4.4	20									785					
801	36.5	10	797			$(\frac{7}{2}^+)$	775		(781)		806					
869	3.2	25					(810)				887					
902	4.2	30				$\frac{5}{2}^+$	$\sim 900$ (broad)				908					
911	2.3	30									947					
944	7.2	40					(906)				965					
1007	7.8	10					963				1036					

TABLE I (Continued)

$E_x$ (keV)	$\sigma(\theta)$ ( $\mu\text{b}/\text{sr}$ )	$\sigma(\theta)_{\text{max}}$ ( $\mu\text{b}/\text{sr}$ )	$\theta_{\text{lab}}$	Present exp.	$^{153}\text{Eu}(p, t)^a$	$E_x$ (keV)	$\sigma(30^\circ)$ ( $\mu\text{b}/\text{sr}$ )	$^{153}\text{Eu}(p, t)^b$	Coulomb exc. <sup>c</sup> ( $\alpha, \alpha'$ ) $E_x$ (keV)	Coulomb exc. <sup>d</sup> ( $p, p'$ ) & ( $\alpha, \alpha'$ ) $E_x$ (keV)	Coulomb exc. <sup>e</sup> ( $c1, c1'$ ) & ( $\alpha, \alpha'$ ) $E_x$ (keV)	Incl. scatt. <sup>f</sup> ( $d, d'$ ) $E_x$ (keV)	Decay of $^{151}\text{Gd}$ $\xi$ $E_x$ (keV)	Decay of $^{151}\text{Gd}$ $\eta$ $E_x$ (keV)
1097		3.7	25											1092
1117		2.5	35						1106					1114
1154		3.4	12.5											1144
1176		7.6	20											1163
1200		12.0	12.5											
1247		3.7	12.5											
1323		1.6	35											
1338		4.4	10											
1353		9.8	15											
1406		20.0	10											
1641		25.0	10											
(doublet?)														

<sup>a</sup> This work. Asterisks indicate  $J^\pi$  assignments from other work.

<sup>b</sup> Reference 28.

<sup>c</sup> Reference 16.

<sup>d</sup> Reference 17.

<sup>e</sup> Reference 18.

<sup>f</sup> References 19 and 20.

<sup>g</sup> Reference 21.

<sup>h</sup> Reference 22.

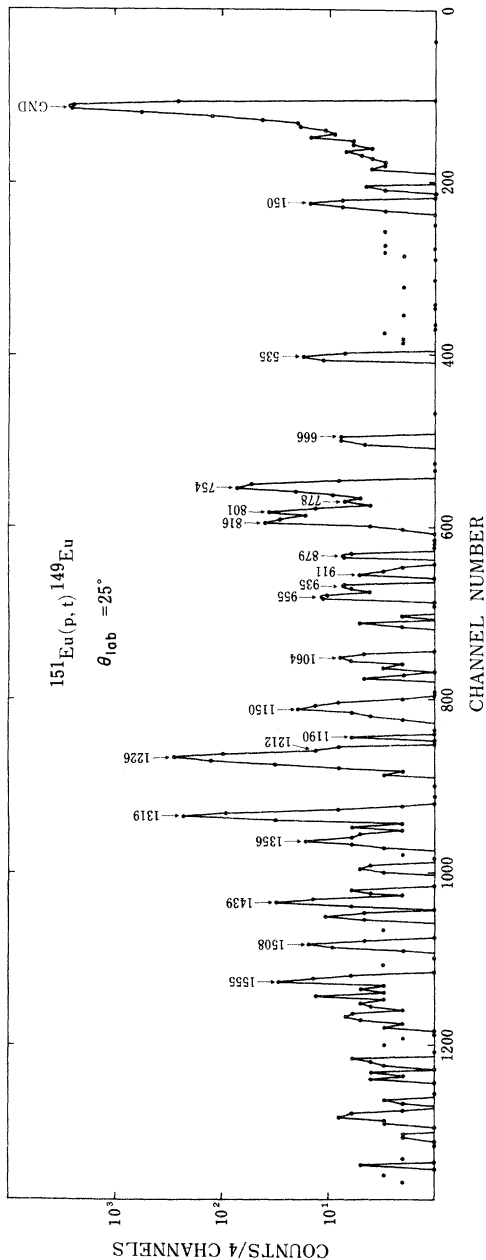


FIG. 3. A typical triton PSD spectrum for the  $^{151}\text{Eu}(p,t)^{149}\text{Eu}$  reaction at  $E_p = 18.5$  MeV and  $\theta_{\text{lab}} = 25^\circ$ . The sums of the counts for every four channels are plotted. Energies for the states are given in keV.

(for  $L=3$ ) is shown in Fig. 5 as an example.

A zero-range DWBA code TWOPAR<sup>38</sup> was used to calculate the angular distributions for each  $L$  value. The optical-model potential used in the DWBA analysis was of the form

$$V(r) = -\frac{V}{1+e^{x_v}} - \frac{iW}{1+e^{x_w}} - \frac{i4W_D e^{x_w}}{(1+e^{x_w})^2} + U_C(R_C A^{1/3}),$$

where  $x_i = (r - R_i A^{1/3})/a_i$  and  $U_C$  is the Coulomb potential of a uniform charge distribution with radius  $R_C$ .

The optical-model parameters used are listed in Table III, where the proton parameters are those taken from Ref. 39, and the triton parameters are from Ref. 40.

Neutron bound-state wave functions were calculated in a real Woods-Saxon potential plus a spin-orbit potential of the Thomas form. The parameters for the neutron bound-state well were radius  $R_v = 1.25$  fm, diffuseness  $a_v = 0.65$  fm, and a spin-orbit strength of 25 times the Thomas term ( $\lambda = 25$ ). The neutron binding energy was taken to be one-half the two-neutron separation energy for each of the transferred neutrons.

As seen in Figs. 2(a) and 4(a), for each residual nucleus there are seven or eight experimental angular distributions which are in good agreement with the calculated  $L=0$  angular distributions. The remaining experimental angular distributions are rather structureless and no angular distribution calculated for a single  $L$  value is able to reproduce the data.

#### IV. DISCUSSIONS

##### A. $^{153}\text{Eu}(p,t)^{151}\text{Eu}$

In this section we will classify each level in the residual nucleus  $^{151}\text{Eu}$  according to the mode of excitation. In Fig. 6 are shown the  $B(E2)\dagger$  values from Coulomb excitation<sup>16-18</sup> and cross sections at  $90^\circ$  from the  $(d,d')$  reaction<sup>19, 20</sup> together with the  $(p,t)$  peak cross sections to each level in  $^{151}\text{Eu}$ . We have also shown in the figure preliminary cross sections at  $\theta_{\text{lab}} = 25^\circ$  for the  $^{150}\text{Sm}(^3\text{He}, d)^{151}\text{Eu}$  reaction from data taken recently at this laboratory.<sup>41</sup> As seen in this figure, there is a strong anticorrelation between the  $B(E2)$  values from Coulomb excitation or  $(d,d')$  cross sections, and the intensities seen in the  $^{153}\text{Eu}(p,t)$  reaction. The Coulomb excitation and the  $(d,d')$  reactions give essentially no strength for the 261, 414, 654, and 801 keV states to which strong or moderately strong  $(p,t)$  transitions have been observed. In contrast, the  $(p,t)$  cross sections are rather weak to the unresolved doublet at 307 keV and the 508 keV state to which Coulomb excitation and the

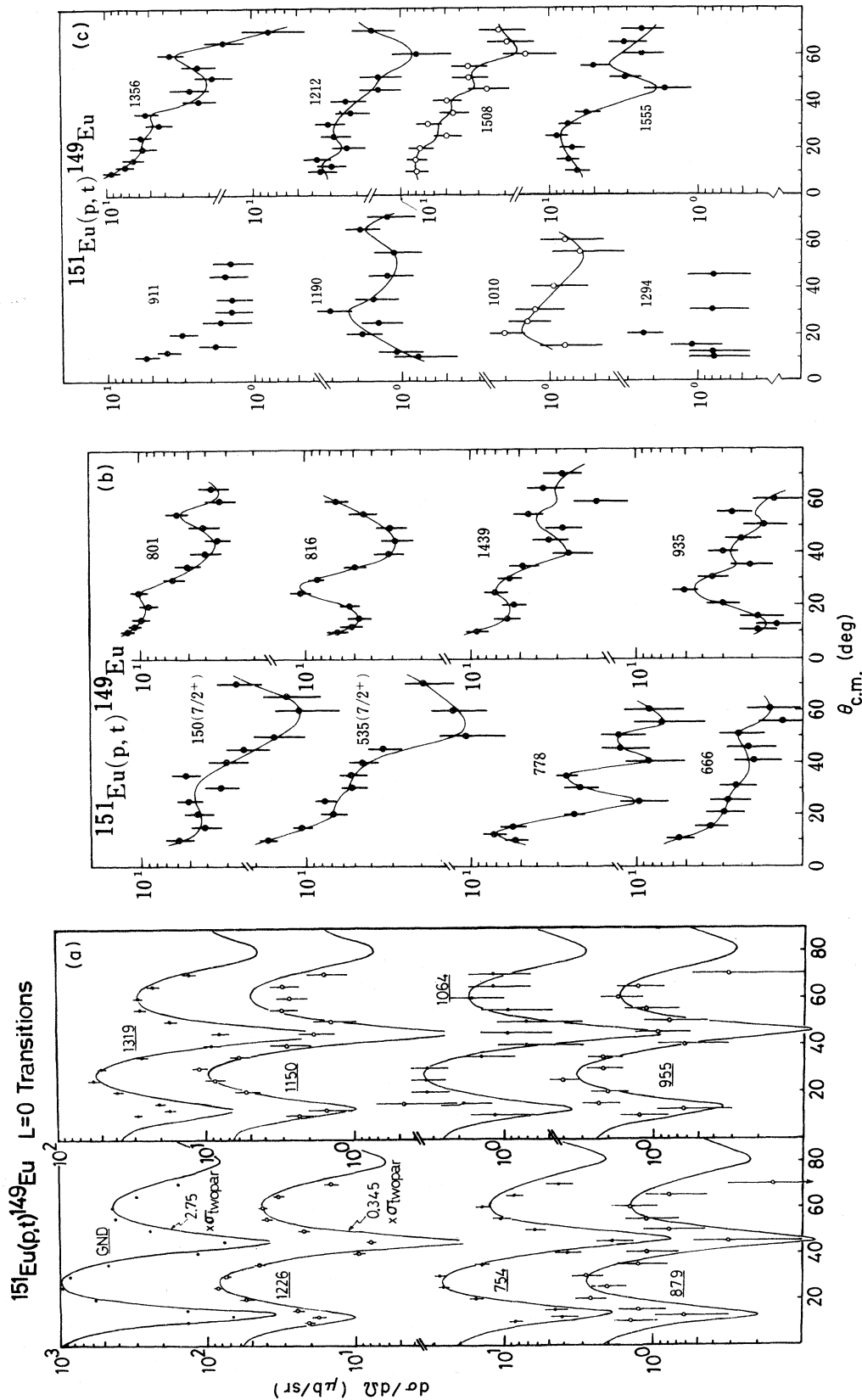


FIG. 4. (a) The  $L=0$  angular distributions for the  $^{151}\text{Eu}(p,t)^{149}\text{Eu}$  reaction at 18.5 MeV. See the caption of Fig. 2 for the details. (b), (c) Angular distributions for the  $^{151}\text{Eu}(p,t)^{149}\text{Eu}$  reaction at 18.5 MeV. Energies are given in keV. Each of the solid curves serves only as a guide to the eye.



TABLE II. Level properties of  $^{149}\text{Eu}$  from the present ( $E_p = 18.5$  MeV) and the  $^{149}\text{Gd}$  decay data. Asterisks indicate  $J^\pi$  assignments from other work. See Sec. IIIA for the errors in the present experiment.

$E_x$ (keV)	$\sigma(\theta)_{\text{max}}$ ( $\mu\text{b}/\text{sr}$ )	$\theta_{\text{lab}}$ (deg)	Present exp.	Decay of $^{149}\text{Gd}$											
				$L$	Ref. 27	Ref. 26	Ref. 25	Ref. 24	Ref. 23						
				$E_x$ (keV)	$J^\pi$	$E_x$ (keV)	$J^\pi$	$E_x$ (keV)	$J^\pi$	$E_x$ (keV)	$J^\pi$	$E_x$ (keV)	$J^\pi$		
0	957.7	25	0	0	$\frac{5^+}{2}$	0	$\frac{5^+}{2}$	0	$\frac{5^+}{2}$	0	$\frac{5^+}{2}$	0	$\frac{5^+}{2}$		
150	6.6	10		149.6	$\frac{1^+}{2}$	149.8	$\frac{1^+}{2}$	150	$\frac{1^+}{2}$	150	$\frac{1^+}{2}$	149.8	$\frac{1^+}{2}$		
				459.9	$\frac{3^+}{2}, \frac{5^+}{2}, \frac{1^+}{2}$							404.0	(+)		
535	17.2	10		496.2	$\frac{11^-}{2}$	496.6	$\frac{11^-}{2}$	497	$\frac{11^-}{2}$	497	$\frac{11^-}{2}$	496.5	$\frac{11^-}{2}$		
666	6.1	10		534.2	$\frac{1^+}{2}$	534.4	$\frac{1^+}{2}$	534	$\frac{3^+}{2}, \frac{5^+}{2}, \frac{1^+}{2}$	535	$\frac{5^+}{2}, \frac{1^+}{2}$	534.3	+		
				666.0	$\frac{5^+}{2}, \frac{1^+}{2}, (\frac{9^+}{2})$	666.6	$\frac{5^+}{2}, \frac{1^+}{2}, \frac{9^+}{2}$	667	$\frac{5^+}{2}, \frac{1^+}{2}, \frac{9^+}{2}$	666	$\frac{5^+}{2}, \frac{1^+}{2}, \frac{9^+}{2}$	666.6	+		
												672.5	(+)		
754	27.5	30	0	748.2	$\frac{1^-}{2}$	749.1	$\frac{5^-}{2}, \frac{1^-}{2}$	750	$\frac{5^-}{2}, \frac{1^-}{2}$	750	$\frac{5^-}{2}, \frac{1^-}{2}$	749.0	$\frac{1^-}{2}$		
778	8.3	12.5			$\frac{5^+}{2}$										
801	13.5	10		794.8	$\frac{9^-}{2}$	795.1	$\frac{9^-}{2}$	796	$\frac{9^-}{2}$	796	$\frac{9^-}{2}$	795.1	$\frac{9^-}{2}$		
816	11.4	25		812.4	$\frac{5^+}{2}, \frac{1^+}{2}, \frac{9^+}{2}$							813.2	(+)		
879	2.9	30	0	875.8	$\frac{3^+}{2}, \frac{5^+}{2}, \frac{1^+}{2}$							877.0	(-)		
911	5.5	10			$\frac{5^+}{2}$										
935	5.5	25		933.3	$\frac{5^+}{2}, \frac{1^+}{2}, \frac{9^+}{2}$			934							
				939.1	$\frac{5^+}{2}, \frac{1^+}{2}$	939.1	$\frac{5^+}{2}, \frac{1^+}{2}, \frac{9^+}{2}$	939	$\frac{5^+}{2}, \frac{1^+}{2}, \frac{9^+}{2}$	940	$\frac{5^+}{2}, \frac{1^+}{2}, \frac{9^+}{2}$	939.3	$\frac{5^+}{2}$		
955	4.1	25	0		$\frac{5^+}{2}$	956.9	+	958				956.9	(-)		
								(963)							
1064	3.3	25	(0)	1097.3	$\frac{5^-}{2}, \frac{1^-}{2}, \frac{9^-}{2}$	1097.8	$\frac{5^-}{2}, \frac{1^-}{2}, \frac{9^-}{2}$	1099				1097.8	(-)		
1150	11.0	30	0		$\frac{5^+}{2}$										
1190	3.2	30			$\frac{5^+}{2}$										
1212	3.7	15			$\frac{5^+}{2}$										
1226	84.4	25	0		$\frac{5^+}{2}$										
1294	2.4	20			$\frac{5^+}{2}$										
1319	57.5	25	0		$\frac{5^+}{2}$										
1356	9.4	10			$\frac{5^+}{2}$										
1439	10.1	10			$\frac{5^+}{2}$										
1508	8.0	15			$\frac{5^+}{2}$							979.7	(-)		
1555	9.0	25			$\frac{5^+}{2}$							1013.2	(-)		
												1097.8	(-)		

~1600

TABLE III. Optical model parameters used in the DWBA calculation. Triton parameters listed are those for  $E_x=1$  MeV in the residual nuclei. Real and volume imaginary well depths for tritons are expressed as

$$V = 165.0 - 0.17E - 6.4 \frac{N-Z}{A} \quad (\text{MeV})$$

and

$$W = 46.0 - 0.33E - 110 \frac{N-Z}{A} \quad (\text{MeV}),$$

where  $E$  is the corresponding laboratory triton energy (MeV).

	$V$ (MeV)	$R_v$ (fm)	$a_v$ (fm)	$W$ (MeV)	$R_w$ (fm)	$a_w$ (fm)	$W_D$ (MeV)	$R_c$ (fm)	Target	Ref.
Protons	57.03	1.17	0.75	1.37	1.32	0.633	9.28	1.30	$^{153}\text{Eu}$	39
	56.78	1.17	0.75	1.37	1.32	0.626	9.16	1.30	$^{151}\text{Eu}$	39
Tritons	162.03	1.20	0.72	24.08	1.40	0.84	0	1.30	$^{153}\text{Eu}$	40
	162.02	1.20	0.72	25.22	1.40	0.84	0	1.30	$^{151}\text{Eu}$	40

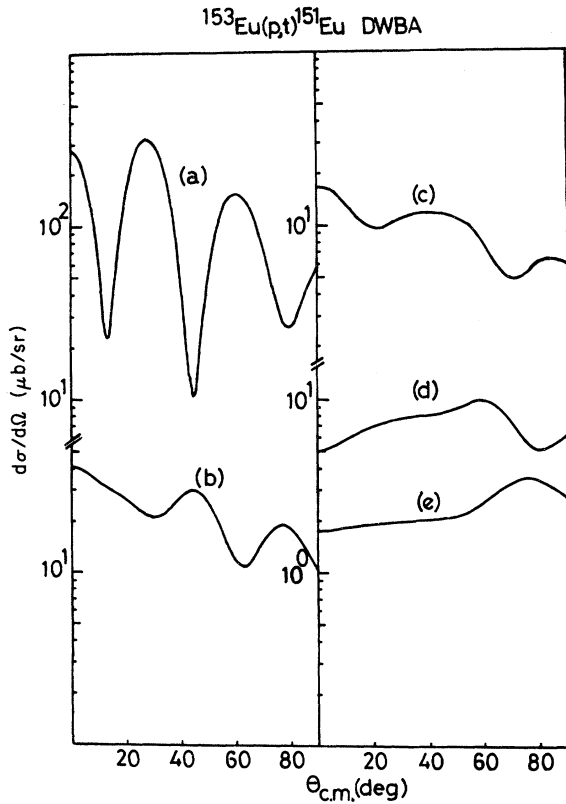


FIG. 5. A sample of DWBA curves for the  $^{153}\text{Eu}(p,t)-^{151}\text{Eu}$  reaction at 18.5 MeV calculated by the program TWOPAR (Ref. 38). Transferred  $L$  values, bound-state wave functions of the transferred neutrons, and the excitation energies in  $^{151}\text{Eu}$  are as follows: (a)  $L=0$ ,  $(2f_{7/2})^2_v$ ,  $E_x=0$ ; (b)  $L=2$ ,  $(2f_{7/2})^2_v$ ,  $E_x=414$  keV; (c)  $L=3$ ,  $(2f_{7/2}, 1i_{13/2})_v$ ,  $E_x=500$  keV; (d)  $L=4$ ,  $(2f_{7/2})^2_v$ ,  $E_x=557$  keV; (e)  $L=6$ ,  $(2f_{7/2})^2_v$ ,  $E_x=1000$  keV.

( $d, d'$ ) reaction show very strong transitions. Coulomb excitation and ( $d, d'$ ) reactions on  $^{151}\text{Eu}$  can be expected to excite strongly states corresponding to collective vibrations around an equilibrium shape similar to that of the mainly spherical ground state. The ( $^3\text{He}, d$ ) reaction will populate states with a large component of a single nucleon coupled to the spherical  $^{150}\text{Sm}$  ground state. The data illustrated in Fig. 6 show very little single-nucleon transfer yield to the four states seen strongly in ( $p, t$ ), namely the 261, 414, 654, and 801 keV levels.

The possibility of these four states arising from two-phonon vibrations (which would also be weak in Coulomb excitation and single-nucleon transfer) is quite small, since the ( $p, t$ ) cross section for two-phonon states is usually of the order of 1–2% of the ground state.<sup>42</sup> The above facts suggest that the four states strongly excited in the ( $p, t$ ) reaction have equilibrium shapes quite different from that of the ground state and are closer to that of the  $^{153}\text{Eu}$  target ground state, the  $\frac{5}{2}^+[413]$  bandhead, which has a prolate shape with  $\delta \approx 0.25$ . Thus it is reasonable to assume that the 261 keV state is the head of a  $\frac{5}{2}^+[413]$  rotational band and that the 654 keV state is the head of a “ $\beta$ -vibrational” band,  $\frac{5}{2}^+[413]\beta$ , with a core similar in structure to the 688 keV  $0^+$  state in  $^{152}\text{Sm}$ .

The states at 414 and 801 keV are populated with intensities of  $\sum_{\theta} \sigma(\theta) / \sum_{\theta} \sigma_{5/2^+}(\theta) = 1/6.9$  and  $1/5.3$ , respectively, relative to their assumed bandheads (the 261 keV state for the 414 keV state and the 654 keV state for the 801 keV state), which are close to that expected for the lowest rotational excitations ( $J = \frac{7}{2}$ ) of the two  $K = \frac{5}{2}$  bands. For example, in  $^{173}\text{Yb}(p, t)^{171}\text{Yb}$ , at  $E_p = 19$  MeV,<sup>36</sup> the

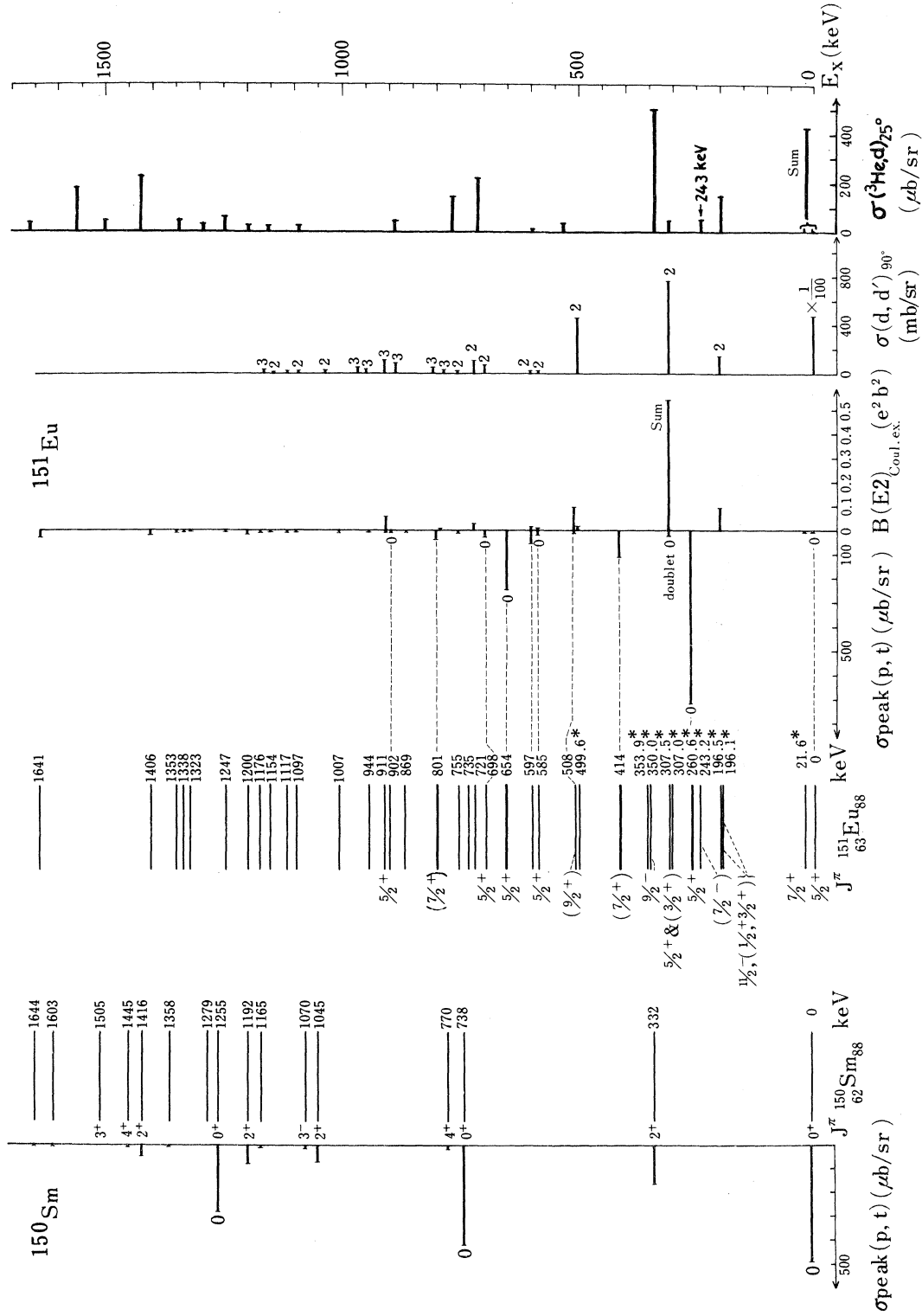


FIG. 6. Known energy levels and transition strengths to  $^{151}\text{Eu}$  and  $^{150}\text{Sm}$ . On the right is shown a comparison of various transition yields  $[(p, t)$  peak cross sections at 18.5 MeV,  $B(E2)_{\text{Coul.}}$  from Coulomb excitations (Refs. 16-18), cross sections at  $90^\circ$  from the  $(d, d')$  reaction (Ref. 19), and cross sections at  $25^\circ$  from the  $(^3\text{He}, \alpha)$  reaction at an incident energy of 28 MeV (Ref. 41)] to  $^{151}\text{Eu}$  levels. On the left are shown the  $(p, t)$  cross sections at 19 MeV for the neighboring even isotones  $^{152}\text{Sm}_{90}(p, t)^{150}\text{Sm}_{88}$  (Ref. 7).  $L=0$  transitions are indicated as "0" on the bars. For  $(d, d')$  reaction, quadrupole (2) and octupole (3) transitions are indicated. Excitation energies of  $^{151}\text{Eu}$  levels shown are mostly from the present experiment except those with asterisks which are the averages of the four  $\gamma$ -ray experiments (Refs. 17, 18, 21, and 22). See Table I for the sources of the spins and parities shown. The level scheme of  $^{150}\text{Sm}$  was taken from Ref. 7.

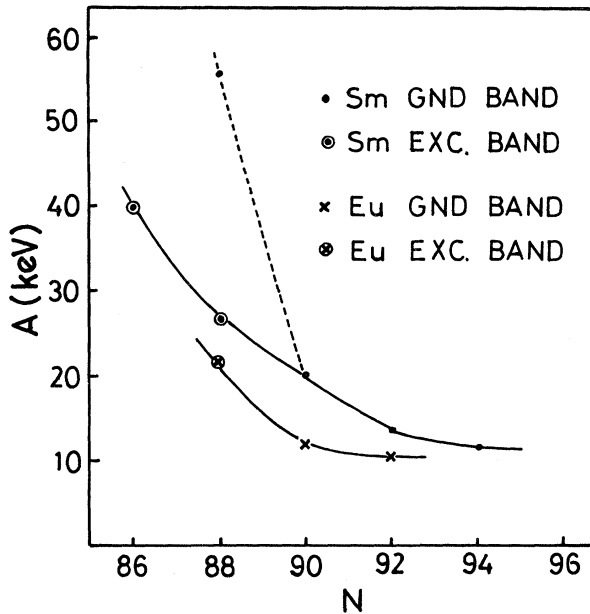


FIG. 7. Systematics of rotational parameter  $A$  for the known ground and excited deformed bands of Sm (Ref. 7) and Eu against neutron number. Solid lines connect  $A$  values for deformed bands.

$\frac{5}{2}^-$  and  $\frac{7}{2}^-$  members of the favored  $\frac{5}{2}^-$ [512] band are excited with a ratio  $\frac{\sum_{\theta} \sigma_{7/2}^-(\theta)}{\sum_{\theta} \sigma_{5/2}^-(\theta)} = 1/5.4$ , and in  $^{161}\text{Dy}(p,t)^{159}\text{Dy}$  the favored  $\frac{5}{2}^+$ [642] band shows a ratio  $\frac{\sum_{\theta} \sigma_{7/2}^+(\theta)}{\sum_{\theta} \sigma_{5/2}^+(\theta)} = 1/6.6$  at  $E_p = 18$  MeV.<sup>43</sup> In previous cases where excited deformed bands have been seen in spherical even-even nuclei their first rotational states have been observed with similar intensity ratios ( $\sim 1/5$  for  $^{150}\text{Sm}$  and  $\sim 1/3.6$  for  $^{148}\text{Sm}$ ). If the 414 and 801 keV states are tentatively assigned as the  $\frac{7}{2}^+$  members of the two  $K^\pi = \frac{5}{2}^+$  bands, their rotational parameters  $A$  can be compared with those of bands in the neighboring Sm and Gd nuclei. The 261 keV band would then have  $A = 21.9$  keV, and the 654 keV band  $A = 21.0$  keV. These are quite close to the  $A$  values for the neighboring even deformed nuclei  $^{152}\text{Sm}_{90}$  ( $A = 20.3$  keV for the ground band and  $A = 21.0$  keV for the “ $\beta$  band” at 685 keV) and  $^{154}\text{Gd}_{90}$  ( $A = 20.5$  keV for the ground band), but are somewhat larger than for the  $^{153}\text{Eu}$  ground-state band ( $A = 11.9$  keV). In Fig. 7 we have plotted  $A$  values for the known ground and excited deformed bands against neutron number. It is seen from this figure that the Eu deformed sequence follows a pattern similar to that observed for the Sm ground and excited bands through the transitional region. Furthermore, the angular distributions of the 414 and 801 keV states are quite similar, as can be seen in Fig. 2(b). These angular distributions have a structure fairly similar to the experimental

and theoretical  $(p, t)$  angular distributions for the  $2^+$  members of the ground-state rotational bands in deformed nuclei.<sup>33</sup>

From this evidence, admittedly circumstantial, it seems reasonable to make the 414 and 801 keV states the  $\frac{7}{2}^+$  members of the  $K^\pi = \frac{5}{2}^+$  bands, although it is necessary to confirm this assignment by studying the  $\gamma$  decay of these states. Such an experiment is now in progress. Higher members of these bands cannot be assigned with any certainty but the state seen in  $(p, t)$  at 597 keV has the correct energy and intensity to be the  $\frac{9}{2}^+$  member of the  $\frac{5}{2}^+$ [413] band starting at 261 keV.

Assuming the above assignments are correct, it is interesting to note that the effect of the odd proton in  $^{151}\text{Eu}$  is to lower the deformed state by almost 1 MeV, from 1255 keV in  $^{150}\text{Sm}$  to 261 keV in  $^{151}\text{Eu}$ , and to decrease the rotational parameter  $A$  from 27 keV in  $^{150}\text{Sm}$  to 21.9 keV in  $^{151}\text{Eu}$ . However, the energy measured from the ground state of the 654 keV “ $\beta$  vibration” in  $^{151}\text{Eu}$  is near that of the low  $0^+$  states in both of the neighboring spherical and deformed nuclei, namely, 740 keV for  $^{150}\text{Sm}$  and 685 keV for  $^{152}\text{Sm}$ . Evidently the energy of the lowest  $J=0$  vibration in these transitional nuclei is relatively independent of the average deformation of the ground state. If however the energy of the “ $\beta$  vibration” (654 keV) is measured from the bandhead of the lowest deformed state in  $^{151}\text{Eu}$  (261 keV), its energy is  $\sim 300$  keV lower than for the neighboring even nuclei. In any case, the nature of these states in the 700 keV region of even nuclei is certainly not well understood and it is necessary to postulate large zero-point shape oscillations in the target or residual states to explain their strong population in  $(t, p)$  and  $(p, t)$  reactions.<sup>1-11</sup>

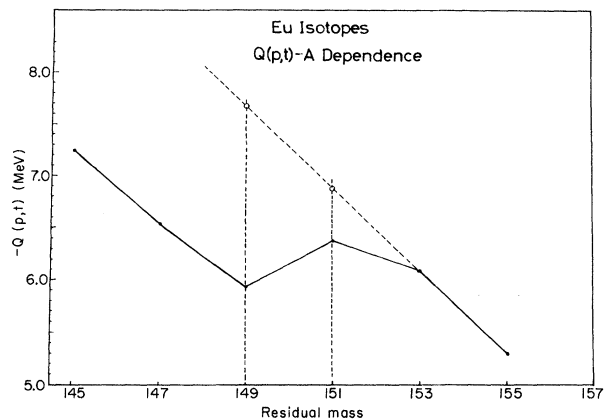


FIG. 8. Residual  $A$  dependence of  $(p, t)$   $Q$  values for Eu isotopes (solid line). The dashed line gives an estimate of the location of deformed states in  $^{149}\text{Eu}$  and  $^{151}\text{Eu}$ .

The expected location of deformed states in the "spherical" nucleus  $^{151}\text{Eu}$  can be determined approximately from the  $(p, t)$   $Q$ -value mass number dependence as shown in Fig. 8. Extrapolation of the  $\text{Eu}(p, t)$   $Q$  value from the deformed side to the lower-mass spherical side indicates that a deformed state is expected at  $\sim 500$  keV in  $^{151}\text{Eu}$  and at  $\sim 1700$  keV in  $^{149}\text{Eu}$ .

For comparison, we have also shown in Fig. 6 the level scheme of the neighboring even isotone of  $^{150}\text{Sm}_{88}$  and the corresponding  $(p, t)$  cross sections at  $E_p = 19$  MeV. It is interesting to note that the summed  $L=0$  cross section ( $E_x \lesssim 1.5$  MeV) is conserved in adding one proton to the Sm core. The summed  $L=0$  cross section ( $E_x \lesssim 1.5$  MeV) at 19 MeV for the residual nucleus  $^{151}\text{Eu}$  is  $1139 \mu\text{b}/\text{sr}$  at  $25^\circ$  which is, within the errors, the same as the value of  $1180 \mu\text{b}/\text{sr}$  at  $25^\circ$  for  $^{150}\text{Sm}$ .

It is also interesting to note that the cross-section ratio in  $^{153}\text{Eu}(p, t)^{151}\text{Eu}$  of the deformed "ground" bandhead (261 keV) relative to the " $\beta$ -vibration" bandhead (654 keV) is 2.94 closer to the  $^{154}\text{Sm}(p, t)^{152}\text{Sm}$  ratio of 3.04 for the  $0^+$  ground relative to the  $0^+$  " $\beta$  vibration" (685 keV) than to the corresponding ratio of 1.18 in  $^{152}\text{Sm}(p, t)^{150}\text{Sm}$  for the ground to  $0^+$  (740 keV) transitions.

By using the combined data on level energies,  $B(E2)$  values, single-nucleon transfer cross sections, and  $(p, t)$  cross sections for both the  $^{151}\text{Eu}$  and  $^{150}\text{Sm}$  levels, we can tentatively classify the  $^{151}\text{Eu}$  levels in addition to the four deformed levels (261, 414, 654, and 801 keV) discussed above. The ground state is predominantly a  $d_{5/2}^{-1}$  (or  $d_{5/2}$ ) proton state and the first excited state (22 keV,  $J^\pi = 7^+$ ) is predominantly a  $g_{7/2}^{-1}$  (or  $g_{7/2}$ ) proton state on a spherical  $^{152}\text{Gd}$  (or  $^{150}\text{Sm}$ ) ground state.<sup>21, 22</sup> The 309 keV state is known to be a doublet ( $J^\pi = \frac{5}{2}^+$  and  $\frac{3}{2}^+$ ), which might explain the departure from a pure  $L=0$  for the angular distribution. The 196 ( $\frac{1}{2}^+$ ), 307 doublet ( $\frac{3}{2}^+$  and  $\frac{5}{2}^+$ ), and 508 ( $\frac{9}{2}^+$ ) keV states which are strongly excited in Coulomb excitation and in the  $(d, d')$  reaction, and weak in  $(p, t)$ , are interpreted as containing a large fraction of the  $d_{5/2} \otimes ^{150}\text{Sm}$  ( $2^+$ ) multiplet. The weak  $L=0$  transition which we see at 307 keV is presumably to the  $\frac{5}{2}^+$  member of the multiplet. The  $\frac{7}{2}^+$  member of the multiplet is missing so far, but in view of its very small  $(p, t)$  cross section there is a possibility that the first excited state (22 keV,  $\frac{7}{2}^+$ ) contains some of the component.

Several degrees of freedom remain to explain the  $L=0$  transitions seen to states at 585, 698, and 902 keV. A  $\frac{5}{2}^+$  member of the expected  $\frac{3}{2}^+[411]$  deformed band, which is known in  $^{153}\text{Eu}$  at 173 keV, would be populated by  $L=0$  transfer if there is mixing of the  $\frac{5}{2}^+[413]$  and  $\frac{3}{2}^+[411]$  bands. On the basis of the single-particle energies, either the

585 or 698 keV state would be a candidate for this state. More speculatively, if the coexistence picture is taken literally we might expect a  $\frac{5}{2}^+$  state in the vicinity of 700 keV to be formed by coupling a  $d_{5/2}$  particle to the  $0^+$  vibration of  $^{150}\text{Sm}$  at 740 keV. Such a state would be comparable in  $(p, t)$  cross section to the  $d_{5/2}$  ground state in view of the fact that the ground and 740 keV  $0^+$  states in  $^{150}\text{Sm}$  are equally populated in the  $(p, t)$  reaction.

The present data on the  $^{153}\text{Eu}(p, t)^{151}\text{Eu}$  reaction show a completely different  $L=0$  strength pattern from the analogous  $(p, t)$  reaction on even- $A$  isotone  $^{152}\text{Sm}_{90}(p, t)^{150}\text{Sm}_{88}$ , where comparable  $L=0$  strengths were seen to all of the three  $0^+$  states in  $^{150}\text{Sm}$  below 1.3 MeV, the ground, 738, and 1255 keV states. As Burke, Løvnhøiden, and Waddington<sup>28</sup> have already noted, a reason for this is that there is a lack of overlap between the target ( $^{153}\text{Eu}$ ) and residual ( $^{151}\text{Eu}$ ) nuclei in two respects, the odd proton and the core. The  $\frac{5}{2}^+[413]$  Nilsson orbit originates from the  $g_{7/2}$  shell-model orbit in its spherical limit and contains only a small fraction ( $\sim 0.25$ ) of the  $d_{5/2}$  shell-model amplitude even at  $\delta \sim 0.25$ . Since the ground state of  $^{151}\text{Eu}$  seems to be a rather good spherical  $d_{5/2}$  proton state, the ground state of  $^{153}\text{Eu}$  ( $\frac{5}{2}^+[413]$ ) has a poor overlap with the ground state of  $^{151}\text{Eu}$ , partly as a result of the difference in the odd-proton orbit. Also, it is known<sup>44</sup> that the change in the intrinsic quadrupole moments between the Eu isotopes is larger than for the two Sm isotopes, which will result in a smaller core overlap factor for the Eu case.<sup>45</sup> The very small ground-state  $(p, t)$  cross section to  $^{151}\text{Eu}$  thus implies a much smaller zero-point oscillation in the  $^{153}\text{Eu}$  and  $^{151}\text{Eu}$  ground states than in the case for the  $^{152}, ^{150}\text{Sm}$  isotopes.

Finally, in the  $(d, d')$  reaction,<sup>19, 20</sup> about six  $L=3$  levels are tentatively identified in the energy region 785–965 keV as the weak coupling octupole multiplet:  $d_{5/2} \otimes ^{150}\text{Sm}$  ( $3^-$ ) or  $d_{5/2}^{-1} \otimes ^{152}\text{Gd}$  ( $3^-$ ). There is no direct correspondence between this multiplet and the levels excited by the  $(p, t)$  reaction, except for weak transitions at 911 and 944 keV.

#### B. $^{151}\text{Eu}(p, t)^{149}\text{Eu}$

In contrast to the  $^{153}\text{Eu}(p, t)^{151}\text{Eu}$  data, there is no unusual feature in the observed  $^{149}\text{Eu}$  level structure. The  $L=0$  transfer strength ( $J^\pi = \frac{5}{2}^+$ ) is concentrated in the ground state, as it is for  $(p, t)$  reactions on even-even nuclei connecting two nuclei with similar coupling schemes. In addition, there are six or seven  $L=0$  transitions ( $J^\pi = \frac{5}{2}^+$ ) to excited states observed. The strongest of these ( $E_x = 1.226$  MeV) carries intensity less than 10%

of the ground-state transition. In Fig. 9, we compare the level scheme and  $(p, t)$  cross-section pattern for  $^{149}\text{Eu}$  with those for the neighboring even isotone  $^{148}\text{Sm}_{86}$ . At an incident proton energy of 19 MeV, the summed  $L=0$  cross section ( $E_x \lesssim 1.5$  MeV) for  $^{149}\text{Eu}$  is  $1168 \mu\text{b}/\text{sr}$  at  $25^\circ$ , which is only 20% lower than the value of  $1395 \mu\text{b}/\text{sr}$  for  $^{148}\text{Sm}$  to the same range of excitation energy. Unfortunately, there are no data available on Coulomb excitation or inelastic scattering on  $^{149}\text{Eu}$  to

compare with the  $(p, t)$  data, since  $^{149}\text{Eu}$  is not stable. The only data on  $^{149}\text{Eu}$  are those from  $\gamma$  or conversion electron spectroscopy on the decay of  $^{149}\text{Gd}^{23-27}$  and it is rather difficult to determine the configurations of the residual levels. Eppley, McHarris, and Kelly<sup>27</sup> have discussed the level structure of the low-lying states and conclude that the ground state and the first excited state ( $E_x = 0.150$  MeV,  $\frac{7}{2}^+$ ) are predominantly  $(2d_{5/2})^{-1}$  and  $(1g_{7/2})^{-1}$  single-proton states, respectively, and

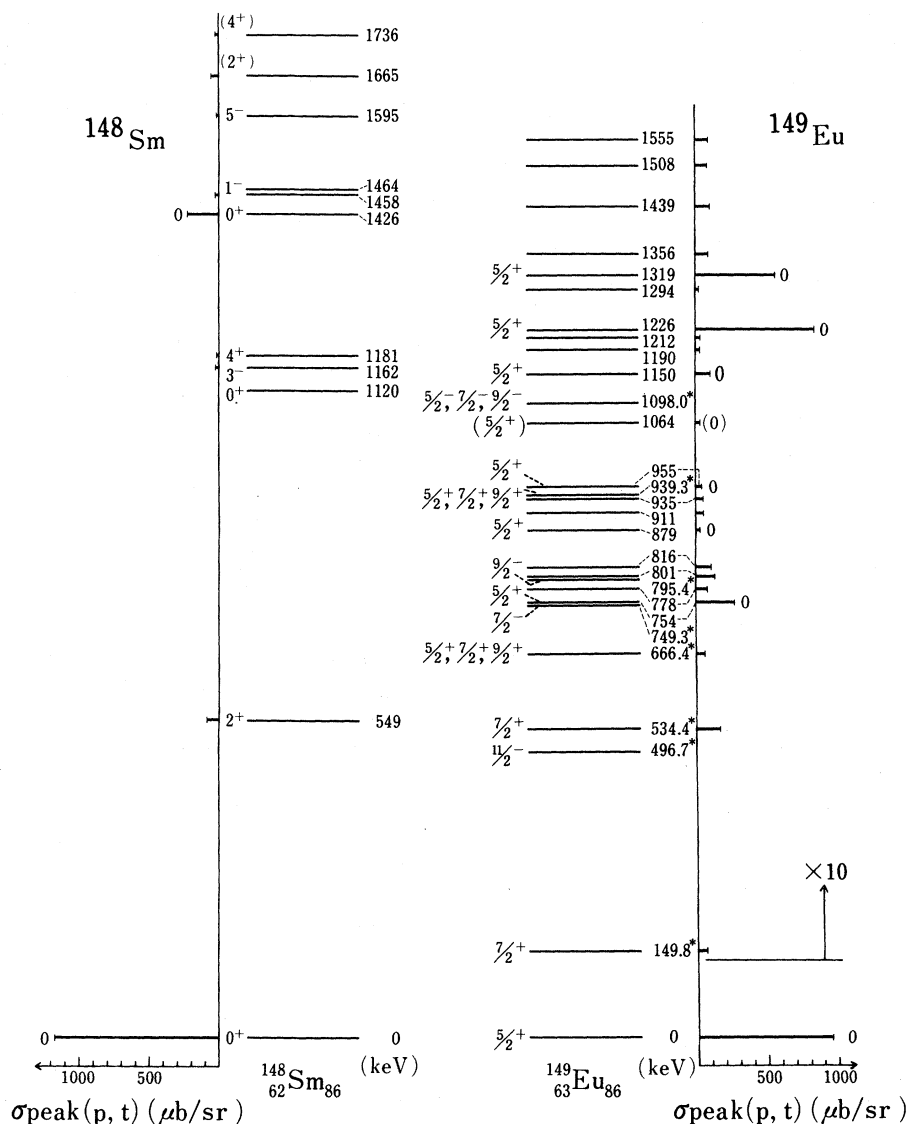


FIG. 9. Known energy levels and a comparison of the cross sections in the  $^{151}\text{Eu}(p, t)^{149}\text{Eu}$  reaction at 18.5 MeV and those in the  $(p, t)$  reaction for the neighboring even isotones  $^{150}\text{Sm}(p, t)^{148}\text{Sm}$  at 19 MeV (Ref. 7).  $L=0$  transitions are indicated as "0" on the bars. Excitation energies of  $^{149}\text{Eu}$  levels with asterisks are the averages of five experiments (Refs. 23-27) on the decay of  $^{149}\text{Gd}$ . Excitation energies of the other  $^{149}\text{Eu}$  levels are determined from the present experiment. See Table II for the sources of the spins and parities shown. The level scheme of  $^{148}\text{Sm}$  was taken from Ref. 7.

not  $K = \frac{5}{2}$  rotational band members. The only other predominantly single-particle state that Eppley *et al.* have identified is an  $h_{11/2}$  state at 496.2 keV, which was not seen in the present experiment.

The  $(p, t)$   $Q$ -value systematics of Fig. 8 suggest the existence of a deformed state at around 1.7 MeV excitation in  $^{149}\text{Eu}$ . We could not find any prominent  $L=0$  transition at this energy region. However, in view of the fact that the deformed states begin at 261 keV in  $^{151}\text{Eu}$ , as compared to ~500 keV estimated from the  $Q$  values, we might expect the deformed  $^{149}\text{Eu}$  states to be somewhat lower than 1700 keV. Two fairly strong  $\frac{5}{2}^+$  states at 1.226 MeV (~9% of the ground state) and 1.319 MeV (~6% of the ground state), may be due to the fractionation of a deformed bandhead. As seen in Fig. 9, the 1.426 MeV  $0^+$  state in  $^{148}\text{Sm}$ , which was identified by Debenham and Hintz<sup>7</sup> as an excited rotational bandhead, is close to the above two  $\frac{5}{2}^+$  states in excitation energy, and its  $(p, t)$  cross section (217  $\mu\text{b}/\text{sr}$  at  $25^\circ$ ) is comparable to the estimated sum of the  $(p, t)$  cross sections of the above two states (170  $\mu\text{b}/\text{sr}$  at  $25^\circ$ ) in  $^{149}\text{Eu}$  at the same incident energy. In contrast to the  $^{153}\text{Eu}$ - $(p, t)^{151}\text{Eu}$  reaction, the lowest odd-proton states in the target ( $^{151}\text{Eu}$ ) and the residual ( $^{149}\text{Eu}$ ) nucleus are both predominantly  $(2d_{5/2})^{-1}$  states, and hence the overlap of the odd-proton part is good. Thus, the  $L=0$  strength to the excited rotational bandhead in  $^{149}\text{Eu}$ , if it exists, would be similar to that in the corresponding even- $A$  core  $(p, t)$  reaction,  $^{150}\text{Sm}_{88}(p, t)^{148}\text{Sm}_{86}$ .

## V. SUMMARY AND CONCLUSIONS

The shape transitional aspects of the odd-mass Eu isotopes,  $^{151}\text{Eu}_{88}$  and  $^{149}\text{Eu}_{86}$ , have been investigated with the  $(p, t)$  reaction at  $E_p = 18.5$  and 19.0

MeV. A number of new levels were found in both  $^{151}\text{Eu}$  and  $^{149}\text{Eu}$ . A number of  $L=0$  transitions were unambiguously identified in both nuclei, indicating the existence of seven  $\frac{5}{2}^+$  states in  $^{151}\text{Eu}$  and seven or eight  $\frac{5}{2}^+$  states in  $^{149}\text{Eu}$ .

In  $^{151}\text{Eu}$ , whose ground state is known to be predominantly a spherical  $d_{5/2}^{-1}$  state, several deformed states, 261 ( $\frac{5}{2}^+$ ), 414 ( $\frac{7}{2}^+$ ), 654 ( $\frac{5}{2}^+$ ), and 801 ( $\frac{7}{2}^+$ ) keV have been strongly excited, while the ground state has shown a vanishingly small cross section. The  $\frac{7}{2}^+$  assignments are tentative and are based mainly on  $(p, t)$  cross-section and moment of inertia systematics. These deformed states have not been seen in Coulomb excitation or  $(d, d')$  reactions, both of which are expected to excite strongly the collective shape vibrations of the spherical ground state. The above experimental data, together with the energy systematics in the neighboring deformed even- $A$  Sm isotopes and the known configuration of the  $^{153}\text{Eu}$  ground state, indicate that the 261 keV,  $\frac{5}{2}^+$  state is the head of a  $\frac{5}{2}^+[413]$  rotational band with its  $\frac{7}{2}^+$  member tentatively identified at 414 keV, and, possibly, its  $\frac{9}{2}^+$  member at 597 keV. The 654 keV,  $\frac{5}{2}^+$  state is probably the head of a  $\frac{5}{2}^+[413]$ , "β band," with its  $\frac{7}{2}^+$  member tentatively at 801 keV.

The neighboring odd- $A$  isotope of  $^{149}\text{Eu}$ , in contrast, has shown the usual  $(p, t)$  pattern of a strong  $L=0$  ground state ( $\frac{5}{2}^+$ ) and weakly excited states, indicating similar coupling schemes are involved in the ground states of the target ( $^{151}\text{Eu}$ ) and the residual ( $^{149}\text{Eu}$ ) nuclei.

One of us (H.T.) would like to thank Professor B. Bayman and Professor N. Onishi for useful conversations concerning the theoretical interpretation of the present data.

\*Work supported in part by the U. S. Atomic Energy Commission.

†Present address: Department of Applied Physics, Tokyo Institute of Technology, Meguro, Tokyo, Japan.

‡Present address: Schuster Laboratory, University of Manchester, England.

<sup>1</sup>S. Hinds, J. Bjerregaard, O. Hansen, and O. Nathan, Phys. Lett. **14**, 48 (1965).

<sup>2</sup>J. H. Bjerregaard, O. Hansen, and O. Nathan, Nucl. Phys. **86**, 145 (1966).

<sup>3</sup>J. R. Maxwell, G. M. Reynolds, and N. M. Hintz, Phys. Rev. **151**, 1000 (1966).

<sup>4</sup>W. McLatchie, J. E. Kitching, and W. Darcey, Phys. Lett. **30B**, 529 (1969).

<sup>5</sup>W. McLatchie, W. Darcey, and J. E. Kitching, Nucl. Phys. **A159**, 615 (1970).

<sup>6</sup>P. Debenham and N. M. Hintz, Phys. Rev. Lett. **25**, 44 (1970).

<sup>7</sup>P. Debenham and N. M. Hintz, Nucl. Phys. **A195**, 385 (1972).

<sup>8</sup>D. G. Fleming, C. Gunther, G. B. Hagemann, B. Herskind, and P. O. Tjøm, Phys. Rev. Lett. **27**, 123 (1971).

<sup>9</sup>T. W. Elze, J. S. Boyno, and J. R. Huizenga, Nucl. Phys. **A187**, 473 (1972).

<sup>10</sup>R. Chapman, W. McLatchie, and J. E. Kitching, Phys. Lett. **31B**, 292 (1970).

<sup>11</sup>R. Chapman, W. McLatchie, and J. E. Kitching, Nucl. Phys. **A186**, 603 (1972).

<sup>12</sup>K. Yagi, K. Sato, Y. Aoki, T. Udagawa, and T. Tamura, Phys. Rev. Lett. **29**, 1334 (1972).

<sup>13</sup>K. Kumar and M. Baranger, Nucl. Phys. **A110**, 529 (1968).

<sup>14</sup>R. Winkler, Phys. Lett. **16**, 156 (1965).

<sup>15</sup>G. G. Seaman, E. M. Bernstein, and J. M. Palms, Phys. Rev. **161**, 1223 (1967).

<sup>16</sup>D. A. Zavadil and R. Graetzer, Nucl. Phys. **A146**, 259

- (1970).
- <sup>17</sup>T. Lewis and R. Graetzer, Nucl. Phys. A162, 145 (1971).
- <sup>18</sup>J. E. Thun and T. R. Miller, Nucl. Phys. A193, 337 (1972).
- <sup>19</sup>G. R. Boss, M. A. thesis, Western Michigan University, 1969 (unpublished).
- <sup>20</sup>E. M. Bernstein, G. R. Boss, G. Hardie, and R. E. Shamu, Phys. Lett. 33B, 465 (1970).
- <sup>21</sup>Å. Hoglund and S. G. Malmkog, Nucl. Phys. A138, 470 (1969).
- <sup>22</sup>J. W. Ford, A. V. Ramayya, and J. J. Pinajian, Nucl. Phys. A146, 397 (1970).
- <sup>23</sup>B. Harmatz and T. H. Handley, Nucl. Phys. 81, 481 (1966).
- <sup>24</sup>I. R. Williams, K. S. Toth, and T. H. Handley, Nucl. Phys. 84, 609 (1966).
- <sup>25</sup>J. M. Jaklevic, E. G. Funk, and J. W. Mihelich, Nucl. Phys. 84, 618 (1966).
- <sup>26</sup>I. Adam, K. S. Toth, and R. A. Meyer, Nucl. Phys. A106, 275 (1968).
- <sup>27</sup>R. E. Eppley, Wm. C. McHarris, and W. H. Kelly, Phys. Rev. C 2, 1077 (1970).
- <sup>28</sup>D. G. Burke, G. Lóvhóiden, and J. C. Waddington, Phys. Lett. 43B, 470 (1973).
- <sup>29</sup>H. Taketani, H. L. Sharma, and N. M. Hintz, in *Proceedings of the International Conference on Nuclear Physics, Munich, 1973*, edited by J. de Boer and H. J. Mang (North-Holland, Amsterdam/American Elsevier, New York, 1973), Vol. 1, p. 229.
- <sup>30</sup>P. H. Debenham, D. Dehnhard, and R. W. Goodwin, Nucl. Instrum. 67, 288 (1969).
- <sup>31</sup>Obtained from Oak Ridge National Laboratory, Oak Ridge, Tenn.
- <sup>32</sup>T. Tamura, D. R. Bes, R. A. Broglia, and S. Landowne, Phys. Rev. Lett. 25, 1507 (1970); 26, 156(E) (1971).
- <sup>33</sup>R. J. Ascuitto, N. K. Glendenning, and B. Sørensen, Phys. Lett. 34B, 17 (1971); Nucl. Phys. A183, 60 (1972).
- <sup>34</sup>T. Udagawa, T. Tamura, and T. Izumoto, Phys. Lett. 35B, 129 (1971).
- <sup>35</sup>T. Udagawa and T. Tamura, in Proceedings of the Symposium on two-neutron transfer and pairing excitation, Argonne National Laboratory, 1972 [Argonne National Laboratory Informal Report No. PHY-1972H (unpublished)], p. 193.
- <sup>36</sup>M. A. Oothoudt and N. M. Hintz, Nucl. Phys. A213, 221 (1973).
- <sup>37</sup>N. B. Gove and A. H. Wapstra, Nucl. Data A11, 129 (1972).
- <sup>38</sup>B. F. Bayman, zero-range DWBA Code TWOPAR (unpublished).
- <sup>39</sup>F. D. Becchetti, Jr., and G. W. Greenlees, Phys. Rev. 182, 1190 (1969).
- <sup>40</sup>F. D. Becchetti, Jr., and G. W. Greenlees, in *Proceedings of the Third International Symposium on Polarization Phenomena in Nuclear Reactions, Madison, 1970*, edited by H. H. Barschall and W. Haeberli (Univ. of Wisconsin Press, Madison, Wisconsin, 1971), p. 682.
- <sup>41</sup>H. L. Sharma, H. Taketani, and N. M. Hintz, in J. H. Williams Laboratory of Nuclear Physics, University of Minnesota Annual Report, 1974 (unpublished), p. 114; and (unpublished).
- <sup>42</sup>For example, at  $E_p = 19$  MeV, the  $(p, t)$  cross section for the 1.133 MeV  $0^+$  state of  $^{106}\text{Pd}$  is 2% of the ground-state value [A. W. Kuhfeld and N. M. Hintz, in J. H. Williams Laboratory of Nuclear Physics, University of Minnesota, Annual Report, 1972 (unpublished), p. 77]. In the  $\text{Te}(p, t)$  reaction, the two-phonon  $0^+$  states are populated with less than 1% of the ground-state cross section [R. Seltz and N. M. Hintz, in J. H. Williams Laboratory of Nuclear Physics, University of Minnesota, Annual Report, 1972 (unpublished), p. 88].
- <sup>43</sup>G. Hagemann, N. M. Hintz, P. Kleinheinz, and M. A. Oothoudt, in J. H. Williams Laboratory of Nuclear Physics, University of Minnesota, Annual Report, 1972 (unpublished), p. 95.
- <sup>44</sup>V. S. Shirley, in *Hyperfine Interactions in Excited Nuclei*, edited by G. Goldring and R. Kalish (Gordon and Breach, New York, 1971), p. 1255.
- <sup>45</sup>T. Takemasa, M. Sakagami, and M. Sano, Phys. Lett. 37B, 473 (1971).